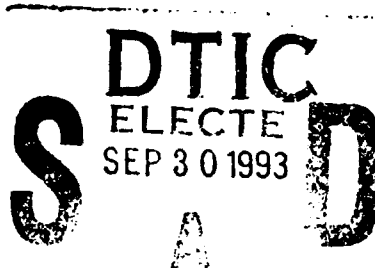




**AN EQUATION OF STATE FOR SHOCK IN  
HOMOGENEOUS MATERIALS AND COMPARISON  
TO SHOCK DATA**

2

J.H. Shively  
C. Stein  
R. Robertson



August 1993

Final Report

---

APPROVED FOR PUBLIC RELEASE; DISTRIBUTION IS  
UNLIMITED.

---

93-22562



**PHILLIPS LABORATORY**  
Space and Missiles Technology Directorate  
AIR FORCE MATERIEL COMMAND  
KIRTLAND AIR FORCE BASE, NM 87117-5776

---

This final report was prepared by the Phillips Laboratory, Kirtland Air Force Base, New Mexico, under Job Order 2864TR05. The Laboratory Project Officer-in-Charge was Jon H. Shively (VTSI).

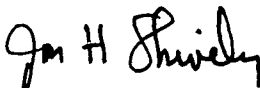
When Government drawings, specifications, or other data are used for any purpose other than in connection with a definitely Government-related procurement, the United States Government incurs no responsibility or any obligation whatsoever. The fact that the Government may have formulated or in any way supplied the said drawings, specifications, or other data, is not to be regarded by implication, or otherwise in any manner construed, as licensing the holder, or any other person or corporation; or as conveying any rights or permission to manufacture, use, or sell any patented invention that may in any way be related thereto.


This report has been authored by employees of the United States Government. Accordingly, the United States Government retains a nonexclusive royalty-free license to publish or reproduce the material contained herein, or allow others to do so, for the United States Government purposes.

This report has been reviewed by the Public Affairs Office and is releasable to the National Technical Information Service (NTIS). At NTIS, it will be available to the general public, including foreign nationals.


If your address has changed, if you wish to be removed from the mailing list, or if your organization no longer employs the addressee, please notify PL/VTSI, Kirtland AFB, NM 87117-6008 to help maintain a current mailing list.

This report has been reviewed and is approved for publication.

  
JON H. SHIVELY  
Project Officer

  
CHARLES STEIN, GM-14  
Chief, Space Environment  
Interaction Branch

FOR THE COMMANDER

  
EUGENE R. DIONNE, Colonel, USAF  
Director, Space and Missiles Technology  
Directorate

DO NOT RETURN COPIES OF THIS REPORT UNLESS CONTRACTUAL OBLIGATIONS OR NOTICE ON A SPECIFIC DOCUMENT REQUIRES THAT IT BE RETURNED.

REPORT DOCUMENTATION PAGE			Form Approved OMB No. 0704-0188	
Public reporting burden for this collection of information is estimated to average 1 hour per response, including the time for reviewing instructions, searching existing data sources, gathering and maintaining the data needed, and completing and reviewing the collection of information. Send comments regarding this burden estimate or any other aspect of this collection of information, including suggestions for reducing this burden, to Washington Headquarters Services, Directorate for Information Operations and Reports, 1215 Jefferson Davis Highway, Suite 1204, Arlington, VA 22202-4302, and to the Office of Management and Budget, Paperwork Reduction Project (0704-0188), Washington, DC 20503.				
1. AGENCY USE ONLY (Leave blank)	2. REPORT DATE August 1993	3. REPORT TYPE AND DATES COVERED Final 1 May 91 - 30 Aug 92		
4. TITLE AND SUBTITLE AN EQUATION OF STATE FOR SHOCK IN HOMOGENEOUS MATERIALS AND COMPARISON TO SHOCK DATA			5. FUNDING NUMBERS PE: 62302F PR: 2864 TA: TR WU: 05	
6. AUTHOR(S) J.H. Shively*, C. Stein, and R. Robertson				
7. PERFORMING ORGANIZATION NAME(S) AND ADDRESS(ES) Phillips Laboratory Kirtland AFB, NM 87117-5776			8. PERFORMING ORGANIZATION REPORT NUMBER PL-TR-92-1060	
9. SPONSORING / MONITORING AGENCY NAME(S) AND ADDRESS(ES)			10. SPONSORING / MONITORING AGENCY REPORT NUMBER	
11. SUPPLEMENTARY NOTES *California State University-Northridge, School of Engineering and Computer Science, Civil and Industrial Engineering and Applied Mechanics.				
12a. DISTRIBUTION / AVAILABILITY STATEMENT Approved for public release; distribution is unlimited.			12b. DISTRIBUTION CODE	
13. ABSTRACT (Maximum 200 words)  An evaluation of hypervelocity impact data for metals, ceramics, ionic, and polymer materials and water as it leads to an equation of state for solids, is presented. The results indicate that for shock induced pressure, the materials behave as if they are in corresponding states, so that a single equation relates pressure to particle velocity for the entire range of materials investigated. The relationship between shock velocity and particle velocity can be represented by a line with a single slope and with an intercept associated with the bulk sound velocity. Comparisons to solid state theory are made which permit a discussion regarding Gruneisen's constant.				
14. SUBJECT TERMS Hypervelocity Impacts, Shock Equation of State, Shock Date Correlations, Shock Pressure Versus Particle Velocity			15. NUMBER OF PAGES 38	
			16. PRICE CODE	
17. SECURITY CLASSIFICATION OF REPORT Unclassified	18. SECURITY CLASSIFICATION OF THIS PAGE Unclassified	19. SECURITY CLASSIFICATION OF ABSTRACT Unclassified	20. LIMITATION OF ABSTRACT SAR	

CONTENTS

<u>Section</u>		<u>Page</u>
1.0	INTRODUCTION	1
2.0	REVIEW OF SHOCK THEORY	3
3.0	LAW OF CORRESPONDING STATES	6
4.0	EVALUATION OF SHOCK DATA	11
5.0	DISCUSSION	20
	5.1 THE GRÜNEISEN CONSTANT	20
	5.2 PRIETO'S EQUATION OF STATE	29
6.0	CONCLUSIONS	31
7.0	FUTURE WORK	32
	REFERENCES	33

Accession For		
NTIS	CRAI	<input checked="" type="checkbox"/>
DTIC	AD	<input type="checkbox"/>
Unannounced		<input type="checkbox"/>
Justification		
By		
Distribution/		
Availability Codes		
Dist	Avail and/or Special	
A-1		

## FIGURES

<u>Figure</u>		<u>Page</u>
1.	Master curve of normalized pressure for hypervelocity collisions as a function of normalized particle velocity for eight metals.	12
2.	Normalized pressure after hypervelocity collisions versus normalized particle velocity for selected ceramics.	14
3.	Normalized pressure after hypervelocity collisions for other metals.	14
4.	Normalized pressure after hypervelocity collisions versus normalized particle velocity for several polymers.	15
5.	Normalized pressure after hypervelocity collisions versus normalized particle velocity for iron powders.	15
6.	Normalized pressure after hypervelocity collisions versus normalized particle velocity for water.	16
7.	Master plot of Equation 8 for normalized pressure after hypervelocity collisions versus normalized and corrected particle velocity.	17
8.	Comparison of master plot for Equation 8 versus master plot curve.	18
9.	Shock velocity versus particle velocity for several materials.	21
10.	Normalized shock velocity versus normalized particle velocity for several materials.	22
11.	Shock velocity versus particle velocity for aluminum and water.	23
12.	Comparison of effect of the slope of the $U_s - U_p$ on calculated values of the normalized pressure as a function of particle velocity.	24
13.	Reduced pressure versus compression, $\Delta V/V_o$ , for three values of the slope of $U_s - U_p$ curve.	26
14.	Adiabatic bulk modulus predictions for various compressions $\Delta V/V_o$ .	27
15.	Comparison of master plot to Prieto's equation.	30

## 1.0 INTRODUCTION

The effects of the space environment on materials and structures in low-earth orbit are of concern to spacecraft designers. The presence of radiation, charged particles, atomic oxygen, micrometeorites, and space debris represents potential sources of material degradation and damage. The issue of collisions from micrometeorites and space debris is particularly important to predictions of spacecraft survivability in that particles, traveling at hypervelocities in the range of 3 to 15 km/s, represent a serious threat to spacecraft integrity.

Hypervelocity collisions are characterized by the phenomena of shock waves in solids. These phenomena have been the subject of numerous investigations and theoretical studies. Most notable has been the extensive study of shock phenomena by Los Alamos National Laboratory which has been a leader in this field for more than 30 years. The data for the study were obtained by Los Alamos as well as other researchers at the Air Force Weapons Laboratory (now the Phillips Laboratory) and at Sandia National Laboratory.

Attempts have been made by individual researchers to relate the observations to theory. Based on the literature on diverse materials, shock data seem to be independent and unrelated. Thus, any attempt to establish a universal equation of state from the data has failed and the equations developed, to date, contain material parameters which lead to a family of equations with different constants.

The quest for a universal equation of state, while elusive, has value in predicting shock behavior. If a universal equation existed, predictions of shock behavior in hypervelocity regions for untested materials and the extrapolation of the results beyond current experimental capabilities would be possible. Also, extensive and expensive experiments would be needed only to corroborate the predictions rather than establish the phenomena for a specific spacecraft material. Therefore, this study was undertaken with the hope that a single equation could be established which describes the phenomena of

PL-TR--92-1060

shock wave propagation in homogeneous solids. The report presents the results of an effort which appear to be successful in establishing a single equation relating the shock pressure to particle velocity. However, future work is required to address the temperature dependence of this equation of state.

## 2.0 REVIEW OF SHOCK THEORY

A collision of a hypervelocity projectile with a target produces shock waves in the target material. The relationship between the pressure induced by the shock, the volume and energy is called the Hugoniot (Ref. 1). The most common expression for the Hugoniot is the so-called Mie-Gruneisen compression equation of state:

$$P - P_H(V_H) = [(\Gamma(V)/V)][(E - E_H(V_H))] \quad (1)$$

where  $P_H$ ,  $V_H$ , and  $E_H$  are pressure, volume, and energy, respectively, along the Hugoniot and  $\Gamma(V)$  is the Gruneisen constant for the material (Ref. 2).

Assuming that the shock wave propagates as a plane wave, the Hugoniot can be expressed in measurable terms of mass, momentum, and energy as in the following conservation equations:

$$\rho U_s = \rho_o(U_s - U_p) \quad \text{Conservation of Mass} \quad (2)$$

$$P - P_o = \rho_o U_s U_p \quad \text{Conservation of Momentum} \quad (3)$$

$$P U_p = \frac{1}{2} \rho_o U_s U_p^2 + \rho_o U_s (E - E_o) \quad \text{Conservation of Energy} \quad (4)$$

where

- $\rho$  = density
- $U_s$  = shock velocity
- $U_p$  = particle velocity
- $P$  = pressure
- $E$  = energy

and subscript, o, refers to the initial state (undisturbed).

Substituting Equations 1, 2, and 3 into Equation 4 yields

$$E_H - E_o = 1/2 (P_H - P_o)(V_o - V_H) \quad (5)$$

The experimental determination of the Hugoniot requires measuring any two of the following three quantities:  $U_s$ ,  $U_p$ , or  $P$  (see Eqs. 2 and 3).

There are several other important relationships which define various aspects of the shock phenomena. For example, most materials exhibit a linear relationship between the shock velocity and the particle velocity, although the reason for this behavior is not understood.

$$U_s = C + sU_p \quad (6)$$

where  $C \approx$  bulk sound velocity = shock velocity at zero pressure. The bulk sound velocity can be determined from a  $U_s - U_p$  plot where  $C$  is the intercept. The bulk sound velocity in solids is given by Reference 3.

$$C^2 = C_L^2 - (4/3) C_s^2 \quad (7)$$

where

$C_L$  = longitudinal speed of sound

$C_s$  = shear speed of sound

Because the shear velocity in liquids is zero,  $C = C_L$ . However, for solids the shear velocity is significant and Equation 7 applies. Extrapolations to  $U_s$  for  $U_p = 0$  correspond closely to the bulk sound velocity. If the shock velocity is linearly related to the particle velocity, then the following equation is obtained which is convenient for representing shock data.

$$P/(\rho_o C^2) = (U_p/C)(1 + sU_p/C) \quad (8)$$

In the past, many workers in shock testing have associated the slope,  $s$ , with the Grüneisen constant,  $\Gamma$ , which is used in Equation 1. The works of Slater (Ref. 4) and Dugdale and MacDonald (Ref. 5) lead to equations for  $\Gamma$  in terms of the slope,  $s$ . The prediction in Reference 4 is  $s = (\Gamma/2) + 1/2$  and the prediction in Reference 5 is  $s = (\Gamma/2) + 1/3$ . Alder (Ref. 6) hints that there must be a limit to the compression because the shape of the pressure compressed volume curves approaches infinity at a finite volume. He predicts that volume is given by

$$(V/V_o)_{\max} = (s - 1/s) \quad (9)$$

Thus if  $s = 4/3$ , then  $(V/V_o)_{\max} = 1/4$  and  $1 - (V/V_o)_{\max} = 0.75$ . Likewise if  $s = 3/2$ , then  $(V/V_o)_{\max} = 1/3$  and the  $1 - (V/V_o)_{\max} = 2/3$ . If the solid behaves like an ideal gas at very high shock pressures, Alder (Ref. 6) suggests that  $(\Delta V/V_o)_{\max}$  should be 0.75 or therefore,  $s = 4/3$ .

## 3.0 LAW OF CORRESPONDING STATES

The thermodynamics of hypervelocity collisions are governed by conventional thermodynamic variables  $P$ ,  $T$ , and  $V$ . If the phenomena are similar in different materials, one might expect a single equation of state to describe shock. However, Equation 1 suggests that the Hugoniot is controlled by the value of the Grüneisen constant,  $\Gamma$ , which varies from metal to metal. Both Slater and Dugdale developed equations which relate the Grüneisen constant to the slope of the  $U_s$  versus  $U_p$  curve. The slope can also be determined from ultrasonic measurements. In this study the slope will later be shown to be universal. A comparison of the slope values obtained from ultrasonic measurements, from theory by Slater and Dugdale, and this study are presented in Table 1. If the slope is universal, then the Grüneisen constant would be the same for all three metals based on shock measurements and either Slater's or Dugdale's equations. A constant slope implies a common thermodynamic framework to describe shock. One framework used frequently to relate the equation of state of different gases is called the Law of Corresponding States. About 10 years ago Prieto (Refs. 7-11) attempted to work out a detailed thermodynamic framework to describe shock that is based upon the Law of Corresponding States. The work of Prieto is reviewed briefly below.

The Law of Corresponding States broadly states that fluids behave alike when in corresponding states; i.e., when  $n$  thermodynamic variables bear a constant ratio to  $n$  critical values of those same thermodynamic variables. Consider as an example, the Van der Waal's equation of state for a gas. The  $p$ ,  $v$ ,  $T$  relation for a given gas can be represented in terms of reduced variables  $p_r$ ,  $v_r$ , and  $T_r$  which are ratios of  $p$ ,  $v$ , and  $T$  to  $p_c$ ,  $v_c$ , and  $T_c$  respectively, where the subscript  $c$  refers to a critical value of the variable for a particular gas. However, any gas can be represented by the reduced form of the Van der Waal's equation of state as long as  $p_c$ ,  $v_c$ , and  $T_c$  are known for that gas. The Van der Waal's equation becomes

$$(p_r + 3/v_r^2)(3v_r - 1) = 8 T_r \quad (10)$$

Table 1. Comparison of the shock velocity versus particle velocity for three metals.

Material	Source			
	Sound	Slater	Dugdale	Universal Slope
Al	1.54	1.38	1.55	1.35
Cu	1.64	1.33	1.50	1.35
Au	1.85	1.85	2.02	1.35

All gases are said to behave identically when in their corresponding states determined by the critical values,  $p_c$ , etc. While corresponding states may not seem to be precise, nevertheless, this principal has had wide use in the fields of equilibrium and transformation properties of pure substances (Refs. 12-14). The principle of corresponding states has been used, for example, to describe incompressible flow behavior (Ref. 15). For dynamic similarity, the Reynolds number is frequently used. It can be shown that the Reynolds number is the ratio of the fluid velocity to the shear velocity, thus  $R = \text{Inertia}/\text{viscous drag}$  is a constant for two dynamically similar situations. More recently, Prieto (Ref. 7) has applied corresponding states to shock thermodynamics.

The development of a universal equation of state to describe shock has been the subject of extensive research in the last 40 years. Prieto has attempted to develop an equation which relates the shock thermodynamic variables (P, V, and E) to experimental parameters, i.e., particle velocity, shock, compressibility, and density. In so doing he takes advantage of an assumed linear relation between shock velocity and particle velocity. Prieto's development of the equation of state in Reference 8 is summarized below. He defines compression as Z, given by

$$Z = 1 - \rho/\rho_0 = \Delta V/V_0 \quad (11)$$

where  $\rho$  is density and V is volume.

From Equation 2 it also follows that  $Z = U_p/U_s$ . Combining Equations 2, 3, and 4 with 11 gives:

$$P = \rho_0 C^2 Z (1 - sZ)^{-2} \quad (12)$$

Using the principle of corresponding states from Reference 7, Prieto in Reference 8 defines critical ratios

$$Q_2 = K_Q Q_1 \quad (13)$$

where

$$Q = P, Z, \rho, C, s$$

Using the numerals 1 and 2 to refer to materials and substituting them into Equation 12 leads to

$$s_1 Z_1 = s_2 Z_2 = v_r \quad (14)$$

and

$$P_1 / [(\rho_1 C_1^2) / s_1] = P_2 / [(\rho_2 C_2^2) / s_2] = p_r \quad (15)$$

and rewriting Equation 12 becomes

$$p_r = v_r (1 - v_r)^{-2} \quad (16)$$

Thus, Prieto succeeded in expressing pressure and volume in terms of reduced variables. His proof of the validity of Equation 16 lies in its ability to predict experimental values. Prieto made a few comparisons for a few metals which have nearly the same values of  $s$  and he obtained a very close fit to that data (Ref. 7).

Prieto also developed an expression for the temperature dependence of shock (Ref. 8) in terms of reduced variables. He defined

$$T_r = \alpha s T \quad (17)$$

where

- $T_r$  = reduced temperature
- $\alpha$  = the coefficient of linear expansion
- $s$  = the slope of the  $U_s$   $U_p$  curve
- $T$  = the temperature

In Reference 8, Prieto defines a reduced Grüneisen constant,  $(\Gamma)_r$ , so that Equation 1 can be expressed in reduced variables:

$$p_H - p = (\Gamma)_r (e_r - e) \quad (18)$$

where

$$(\Gamma)_r = \Gamma / v_r \quad (19)$$

It is interesting to note that the reduced Grüneisen constant accounts for the volume dependency of  $\Gamma$  (Alder) in Reference 6, i.e., as  $V$  decreases (compression),  $v_r$  increases.

Also  $(\Gamma)_r$  is related to other thermodynamic variables, i.e., heat capacity at constant volume,  $c_v$ , and the compressibility,  $\kappa$ , with  $c_v$  and  $\kappa$  defined in terms of reduced variables. Prieto in Reference 8 defined

$$c_{vr} = [s/(\alpha)C^2]c_v \quad (20)$$

and

$$(\kappa)_r = \rho_o C^2 \kappa/s \quad (21)$$

Applying the reduced variables approach discussed above, Prieto in Reference 8 extended this idea to points along the Hugoniot by using the expression for entropy and the Rankine-Hugoniot equation for conservation of energy. The following differential equation was obtained:

$$(dT_r/dv_r) - (\Gamma)_r T_r = [(v_r)/c_{vr}][1 - v_r]^{-3} \quad (22)$$

This can be integrated along the Hugoniot to obtain the desired equation for temperature

$$T_{rH} = T_{ro} e^{(\Gamma)_r} + 1/c_{vr} (Y^2 e^{- (\Gamma)_r Y})(1 - Y)^{-3} dY \quad (23)$$

where the initial conditions,  $v_r$  and  $\rho_r$ , are zero at  $T_{ro}$  in reference to any other state along the Hugoniot. Prieto in Reference 8 solved the integral for the adiabatic case and obtained

$$T_{ra} = T_{ri} \exp [(\Gamma)_r v_{ra} - v_{ri}] \quad (24)$$

This equation is similar to the equation developed by Walsh and Christian (Ref. 1):

$$T_a(V) = T_i \exp(\Gamma) (V_i - V) \quad (25)$$

The degree to which these equations predict shock behavior is discussed below in terms of the available shock data. Since few temperature data are available, only pressure and volume data will be examined in evaluating the validity of these equations.

## 4.0 EVALUATION OF SHOCK DATA

There is a significant volume of shock data available for evaluating the theory (Refs. 7-11). Recently, it has become possible to produce particle velocities exceeding 10 km/s and, for example, some experiments using an electric gun have achieved particle velocities exceeding 15 km/s. However, most of the available data lie at velocities below 5 km/s. In addition, experimental techniques have improved with the use of laser interferometers and streak cameras to measure velocities. Instrumentation of pressure transducers has also improved.

Shock data are available for a wide variety of materials in the range of 0.01 to 10 km/s. The data, for the most part, have been generated by flyer plate tests in which the plate velocity is measured and the shock velocity is determined through momentum transfer to the target. In a few cases, the pressure is measured during shock by means of transducers while other properties are usually derived from the physics of shock (Eqs. 2 to 4). Selected data from the above reference data banks were electronically scanned into a computer and entered into a computer-based spread sheet program. In most cases the units were converted to a standard set adapted for convenience from older data (Ref. 3). That is, Megabars (Mb), centimeters per second (cm/s), and grams per centimeter cubed ( $\text{g/cm}^3$ ) were used rather than SI units.

The data for shock were manipulated in a special way; viz. the pressure was normalized by dividing by the bulk modulus of sound,  $B_s = \rho_0 C^2$ , and the particle velocity was normalized by dividing by the bulk sound velocity,  $C$ . The results are presented in Figure 1 for eight different metals. The results show that the selections for this normalization of pressure and velocity, while not obvious selections, correct the data to form a master curve. If either normalization step is omitted, the data do not follow a master curve. In retrospect, it is easy to see the validity of the normalization when one considers Prieto's use of corresponding states as a means of describing the shock process. Equation 8 shows that at low ratios of  $U_p/C$ ,  $< 0.1$ , with  $s$  in the range of 1, the second term in the product on the right hand side is  $\sim 1.1$ .

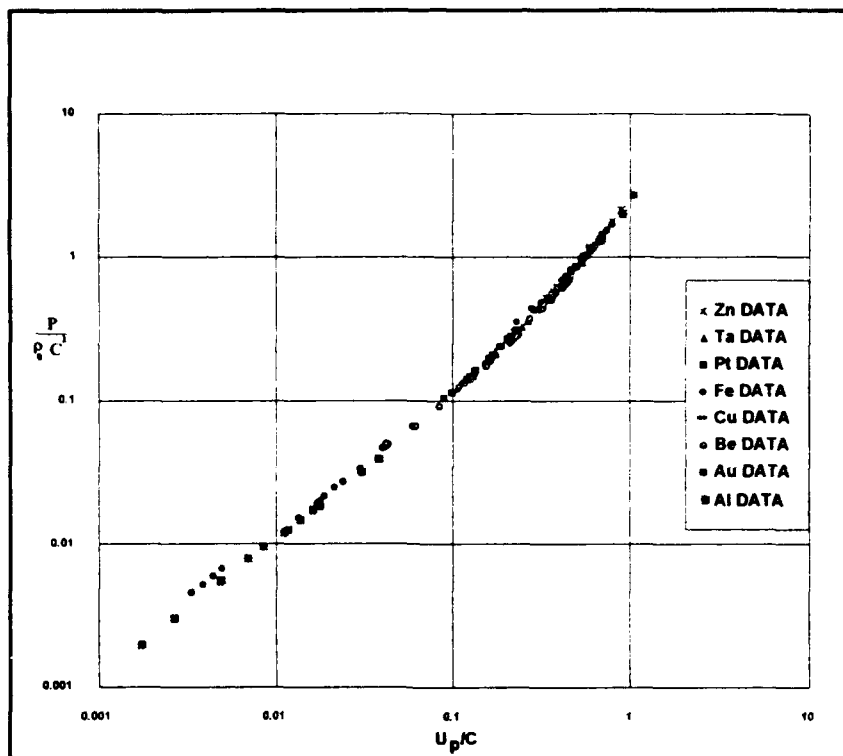


Figure 1. Master curve of normalized pressure for hypervelocity collisions as a function of normalized particle velocity for eight metals.

This means that the normalized pressure approximately equals the normalized particle velocity. Therefore, the relationship  $P/(\rho_0 C^2)$  to  $(U_p/C)$  should be linear with a slope near 1. This appears to be the case as can be seen in Figure 1 for  $U_p/C < 0.1$ .

However, as  $U_p/C$  approaches 0.1, the curve begins to rise as the second term gradually increases above 1. In essence, Equation 8 is a quadratic in  $U_p/C$  in which the second term dominates at values of  $U_p/C > 0.1$ .

What makes Figure 1 remarkable is that eight different metals fit on one curve. Examination of Equation 8 shows that  $s$  is a parameter of the material; i.e., the slopes vary from one material to another. However the agreement shown in Figure 1 suggests that materials have the same slope,  $s$ , as obtained from the  $U_s$  versus  $U_p$  plots. In fact, a

careful review of the literature on shock and the data indicate that materials have slope values which range from 1 to 4. Perhaps the correlation shown in Figure 1 is fortuitous; i.e., the eight metals used in the correlation just happen to have the same slope,  $s$ . To test this, other materials were checked against Figure 1. Ceramic materials such as quartz, corundum, and LiF were compared and each of these ceramics fits the curve presented in Figure 2. By comparing Figure 2 to the master plot, Figure 1, it can be seen that the two graphs superimpose on one another. In addition, three other metals were evaluated by normalizing the pressure and particle velocity and are plotted in Figure 3. This plot also superimposes on Figure 1. Polymers, epoxy, polysulfone, Mylar, Lucite, and Plexiglas were compared to the master curve. The data from polymer materials compare directly with the master plot as can be seen by comparing Figure 4 to Figure 1. Shock data obtained on iron powders ranging in densities from  $4.7 \text{ g/cm}^3$  to the theoretical density of  $7.8 \text{ g/cm}^3$  were also compared to the master curve in Figure 1. These comparisons included correction for both the density and sound velocity changes in iron as a result of the initial powder compaction as can be seen in Figure 5. Finally, shock data obtained on water were normalized. In this case, the bulk sound velocity is the same as the longitudinal sound velocity since the shear sound velocity in water is zero. The graph depicting the behavior of water, shown in Figure 6, also superimposes on top of the master curve. In short, all materials evaluated so far exhibit the same normalized pressure response to a collision by a particle traveling at a normalized velocity.

In a statistical fit of Equation 8, the value of  $s$  was left unassigned in the analysis using a least square routine in the spread sheet program. In the statistical analyses of the data, whether combined with other data or evaluated separately, the slopes,  $s$ , were found to be nearly identical, with  $s$  ranging from 1.12 to 1.16. When all the data are used, the regression coefficient is  $r = 0.9998$  which suggests a high degree of correlation. However, the regression equation specified a slope in log-log space = 1.15. The master plot, corrected through Equation 8, is presented in Figure 7 for some of the same selected metals used in Figure 1. In Figure 8, the data and the correction are plotted

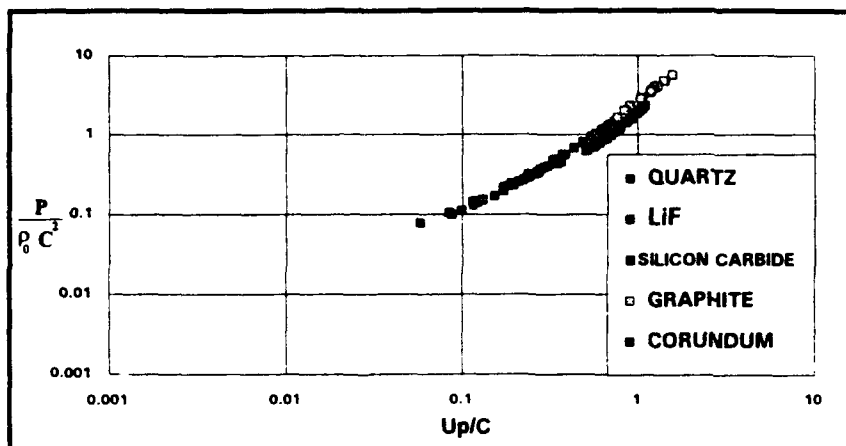


Figure 2. Normalized pressure after hypervelocity collisions versus normalized particle velocity for selected ceramics.

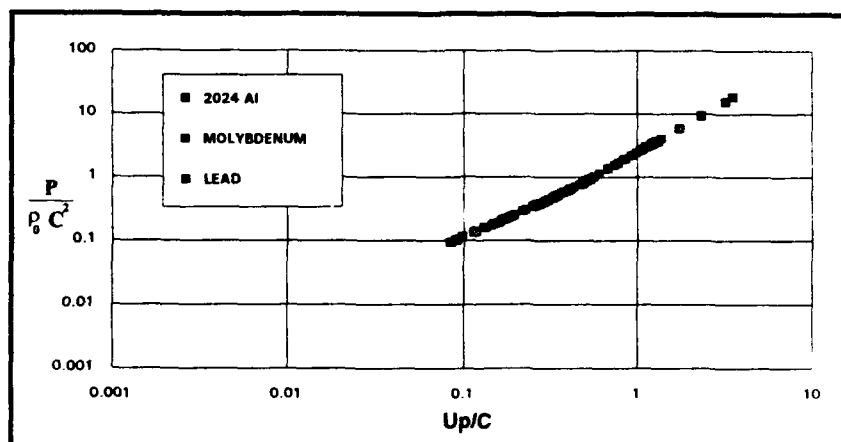


Figure 3. Normalized pressure after hypervelocity collisions for other metals.

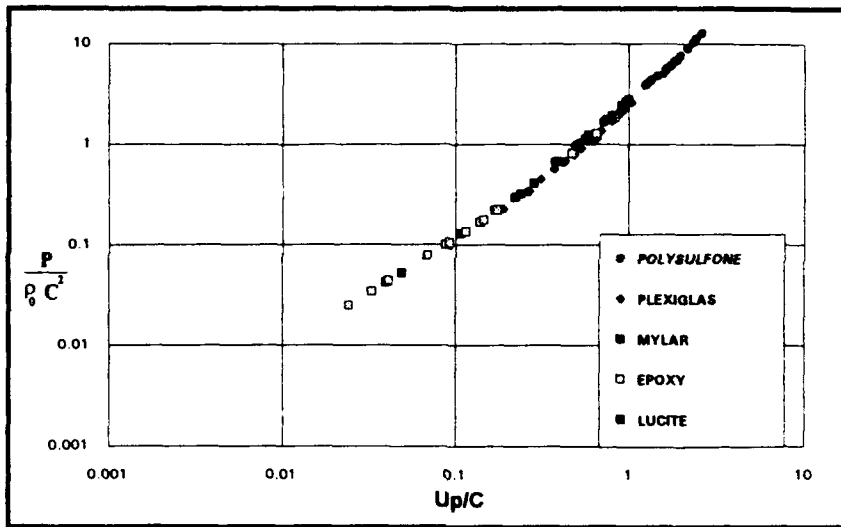


Figure 4. Normalized pressure after hypervelocity collisions versus normalized particle velocity for several polymers.

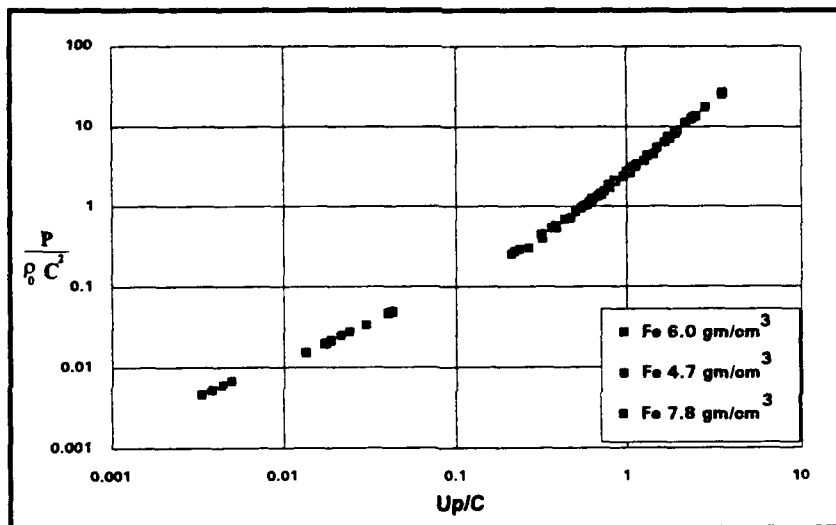


Figure 5. Normalized pressure after hypervelocity collisions versus normalized particle velocity for iron powders.

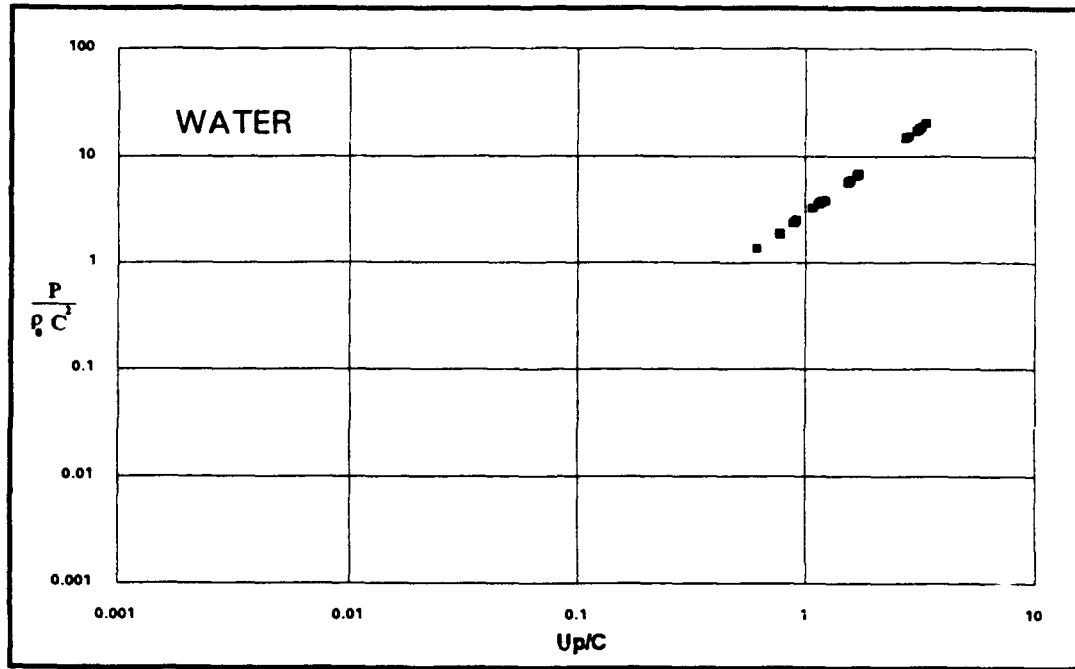


Figure 6. Normalized pressure after hypervelocity collisions versus normalized particle velocity for water.

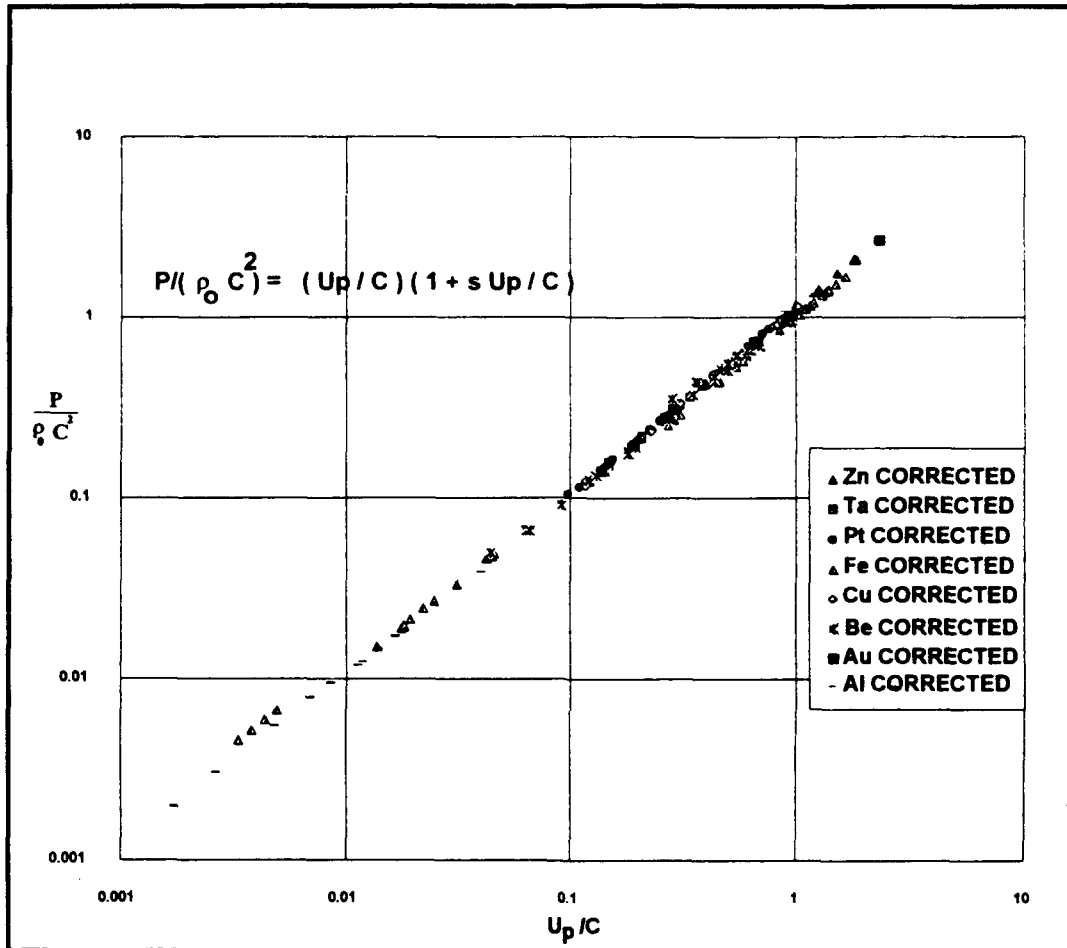


Figure 7. Master plot of Equation 8 for normalized pressure after hypervelocity collisions versus normalized and corrected particle velocity.

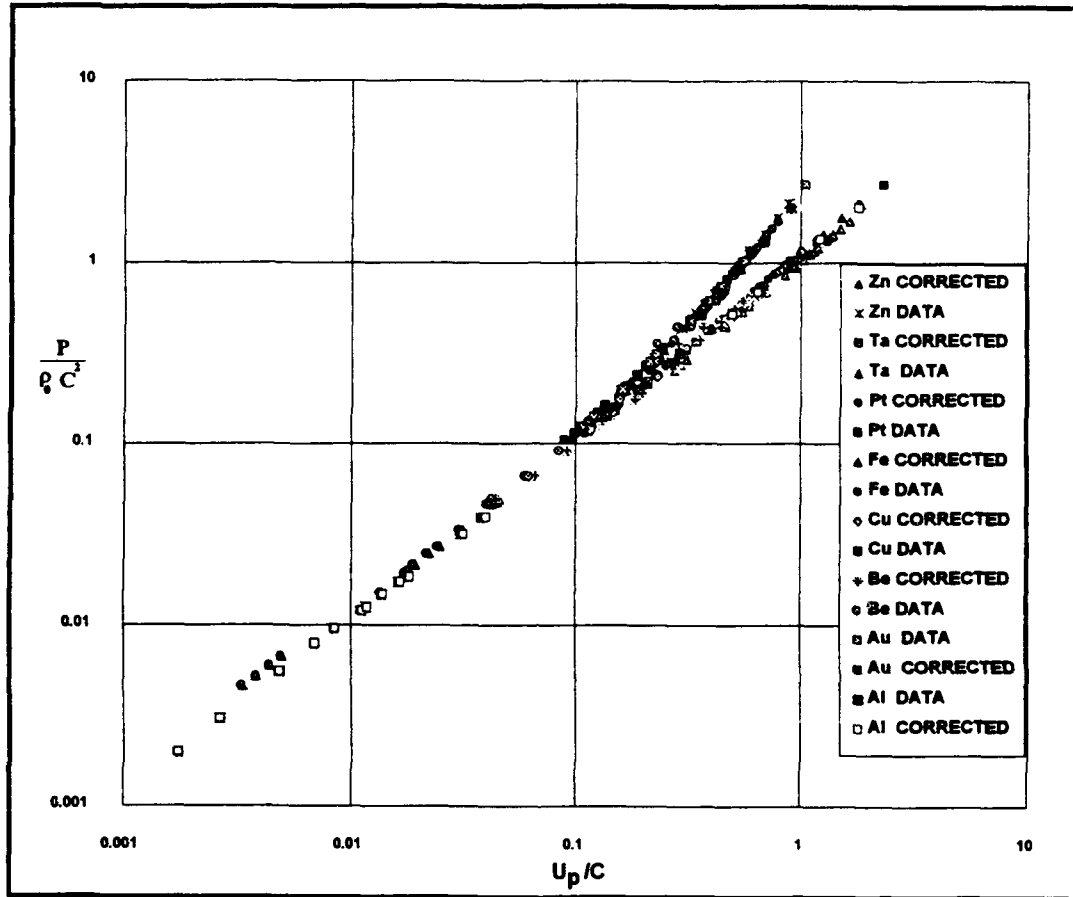


Figure 8. Comparison of master plot for Equation 8 versus master plot curve.

together for comparison purposes. It is easy to see that at values of  $U_p/C < 0.1$ , the curves merge. At values  $U_p/C > 0.1$  the two curves in Figure 8 diverge. It is interesting to note that the corrected graph, which is linear with a slope near 1, agrees with the predictions of Equation 8.

If the correlation of the data shown in Figure 1 or Figure 7 can be verified theoretically and/or by comparisons to all available data, then the figures could be used to interpolate and perhaps to extrapolate the normalized shock pressure-normalized shock particle velocity data to other regimes where data are absent or to other materials for which  $C$  is known. Since the slope of the  $U_s$  versus  $U_p$  curve is known and that the intercept is the bulk sound velocity,  $C$ , a prediction of the shock characteristics can be made without the need for further tests. In other words, Equation 8 combined with Equations 1 through 4 would specify the shock Hugoniot for all homogeneous materials.

## 5.0 DISCUSSION

5.1 THE GRÜNEISEN CONSTANT

One of the inconsistencies in the reported values of slopes, of the  $U_s$ ,  $U_p$  curve, is that they are not as constant as Figure 7 shows and the reported values are generally  $>1.16$ . In addition, since the slope,  $s$ , is related to the Grüneisen constant, whether the Dugdale-MacDonald (Ref. 5) or the Slater (Ref. 4) equation is used, a universal slope means that the Grüneisen constant would be predicted to be the same for all materials used in the correlation of Figure 7. Another problem is that the slope, according to Alder (Ref. 6) (see Eq. 9), would be either 1.33 or 1.5 for maximum compressions of  $1/3$  and  $1/4$ , respectively. The linear regression analysis showed that  $s$  was less than either of these values and equal to 1.16. This implies that the maximum compression  $V/V_0$  is  $1/6$ . This is much smaller than predicted for an ideal gas such as argon.

The question of the differences in the slopes of the  $U_s$  versus  $U_p$  lines for many materials may be partially explained by the uncertainties and limits in the data. In comparing combined data for the  $U_s$  versus  $U_p$  lines for several materials, it is apparent that the slopes are all similar which is not obvious when the slope comparisons are made separately. A comparison of the slopes of several materials is presented in Figure 9. While not perfect because of scatter and an unexplained behavior at very low particle velocities, the slopes of all of the materials presented in Figure 9 bear a striking similarity at high values of  $U_p$ . When data at low values are used or weighted, the difference in the slopes for different materials can be explained. Even more remarkable, when the data for water are plotted on the curve for solids the slope for water compares very closely to that of solids. In fact, the water data also fit the master curves, Figures 1 and 7, for a series of different metals. While comparisons for other fluids were not attempted, several have slopes near 1.35. The results for the materials examined in this study seem to point to a single slope for all plots of shock velocity versus particle velocity when shock occurs at  $U_p > 0.1$  of the bulk sound velocity.

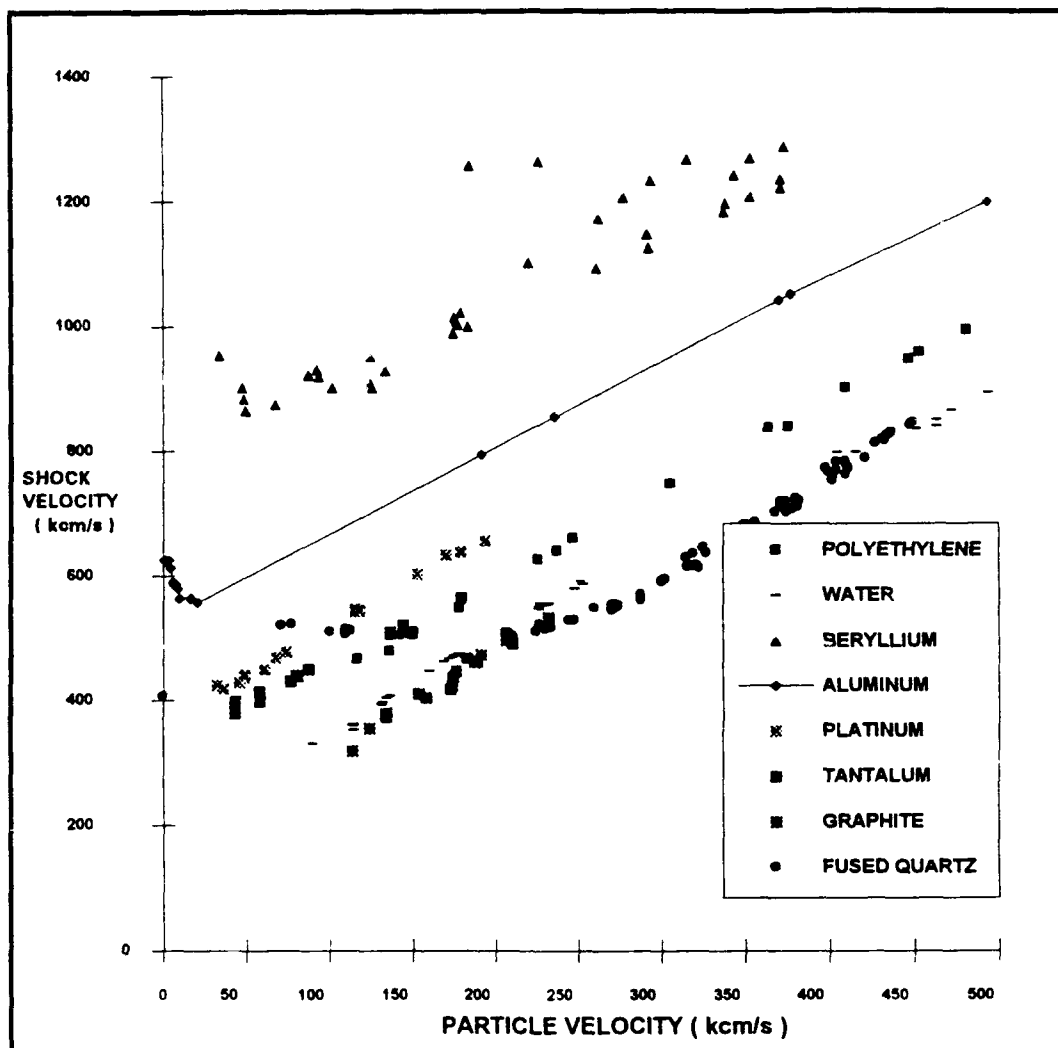


Figure 9. Shock velocity versus particle velocity for several materials.

A comparison of the shock velocity to the particle velocity could be made by normalizing the shock velocity by  $C$ , the bulk sound velocity. This was done in Figure 10 where the data tend to pass through the intercept at 1 because the shock velocity at zero particle velocity is approximately equal to the bulk sound velocity (Eq. 6). While the scatter is large when this comparison is made, the trend of the data suggests a common slope.

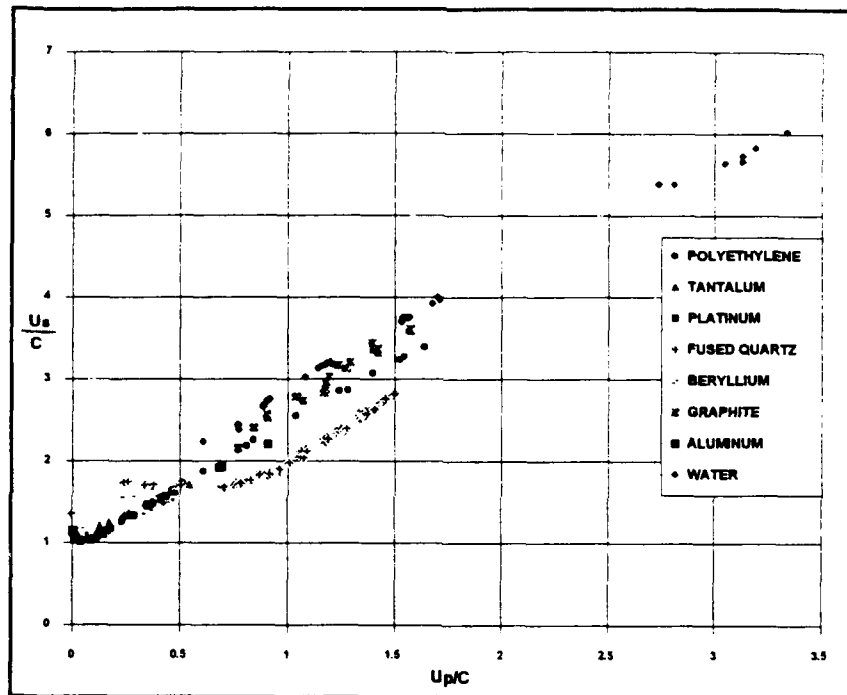


Figure 10. Normalized shock velocity versus normalized particle velocity for several materials.

A comparison of shock velocity data for aluminum and water at high particle velocities shows that the value of the slopes are quite similar (Fig. 11). The theoretical limit for compression given by Alder is  $1/3$  which corresponds to a slope of 1.33. A line with this slope is drawn on Figure 11 to permit comparison to the data. The agreement is remarkable.

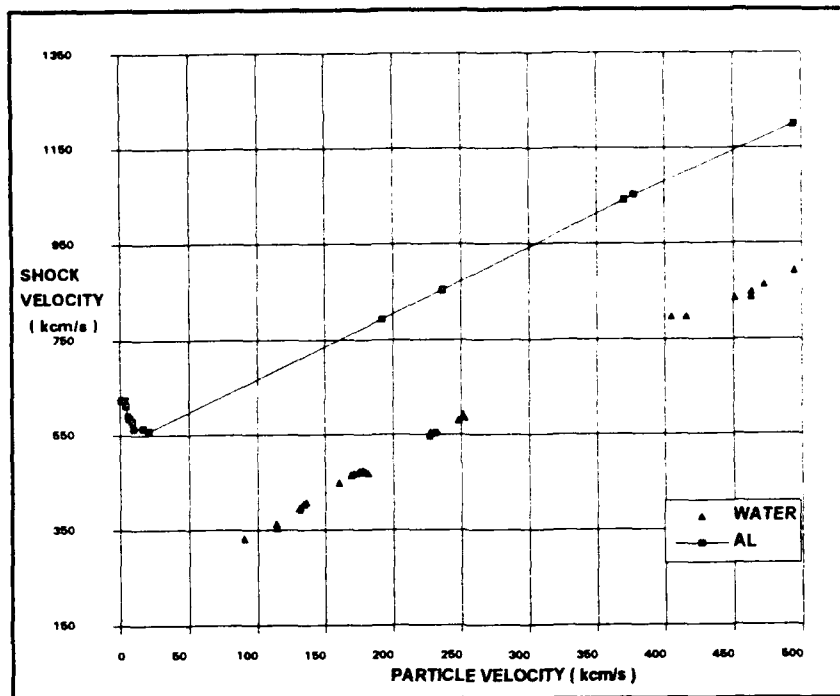


Figure 11. Shock velocity versus particle velocity for aluminum and water.

The statistical evaluation of the selected data, Figure 7, revealed a much smaller value for  $s$  than that obtained with the graphical method, Figures 9 through 11. However, this may be an artifact of plotting the normalized pressure versus the normalized particle velocity on a log-log graph. A linear graph was constructed using Equation 8 for hypothetical values of  $s$  ranging from 0 to 10. The results are presented in Figure 12. As can be seen, the graphical values correlate with the data independently of the value of  $s$ . Moreover, it seems hardly possible to distinguish the effect of the slope 1.16 from 1.35. The predictions lie on top of each other only below  $U_p < 1$ . Looking at the statistics of the comparison little can be said for choosing between the two. However, Equation 8 plotted should have a slope of 1.0. In using the linear regression and allowing  $s$  to vary, the slope of the line for  $s = 1.16$  is 1.16. Thus, the so-called best fit is not the best equation. If  $s$  is set equal to 1.35, the slope is 0.9998. Thus, from the above

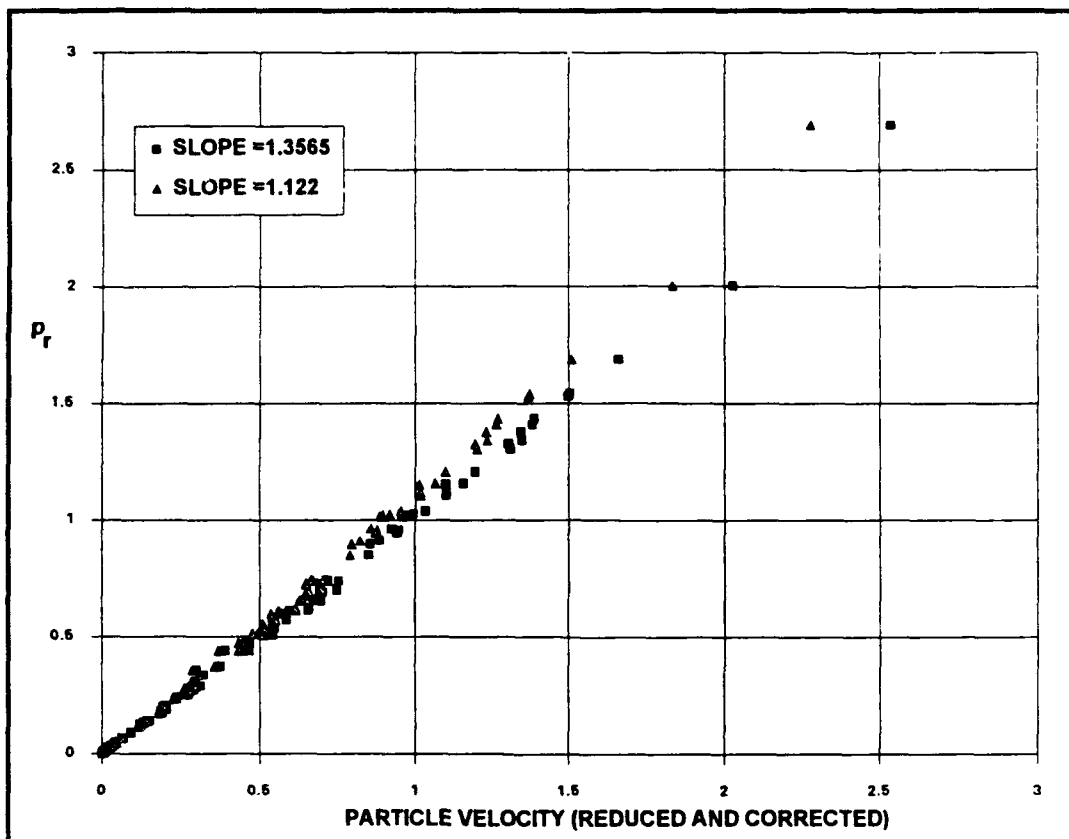


Figure 12. Comparison of effect of the slope of the  $U_s - U_p$  on calculated values of normalized pressure as a function of particle velocity.

discussion of Figures 9 through 11 and the slope of Equation 8 presented in Figures 7 and 12, the value of  $s = 1.335$  is supported rather than 1.16.

The behavior of the reduced pressure as a function of the volume can be obtained from Equation 12 which can be rewritten as

$$P/(\rho_0 C^2) = Z (1 - sZ)^{-2} = p_r \quad (26)$$

This equation can be plotted as a function  $Z$  which is presented in Figure 13. The curves approach infinite pressure as the maximum compression is reached. Thus the slope determines the maximum compression.

Grover, et al, Reference 16, made an extensive study of the bulk modulus of alkali metals using isothermal static data and shock data. Starting with Equation 26, and remembering that  $\rho_0 C^2$  equals the isothermal bulk modulus, and that the adiabatic bulk modulus,  $B_s = -V(dP/dV)_s$ , the following equation can be derived for shock compression:

$$\frac{B_s}{(B_T)_0} = \frac{(1 - Z)(1 - sZ)}{(1 - sZ)^3} \quad (27)$$

where

- $B_s$  = Adiabatic Bulk Modulus
- $s$  = Slope of the  $U_s$  versus  $U_p$  line
- $(B_T)_0$  = Isothermal Bulk Modulus at STP
- $Z$  = Compression =  $\Delta V/V_0$

If  $s$  is a universal constant, as this study shows, then the ratio of  $B_s/B_T$  is dependent only on the compression,  $Z$ , for all materials. This is shown in Figure 14 for four materials. The important point is that from Grover's work the isothermal bulk modulus changes with  $Z$  in an almost identical way as the adiabatic bulk modulus shown in Figure 14. The

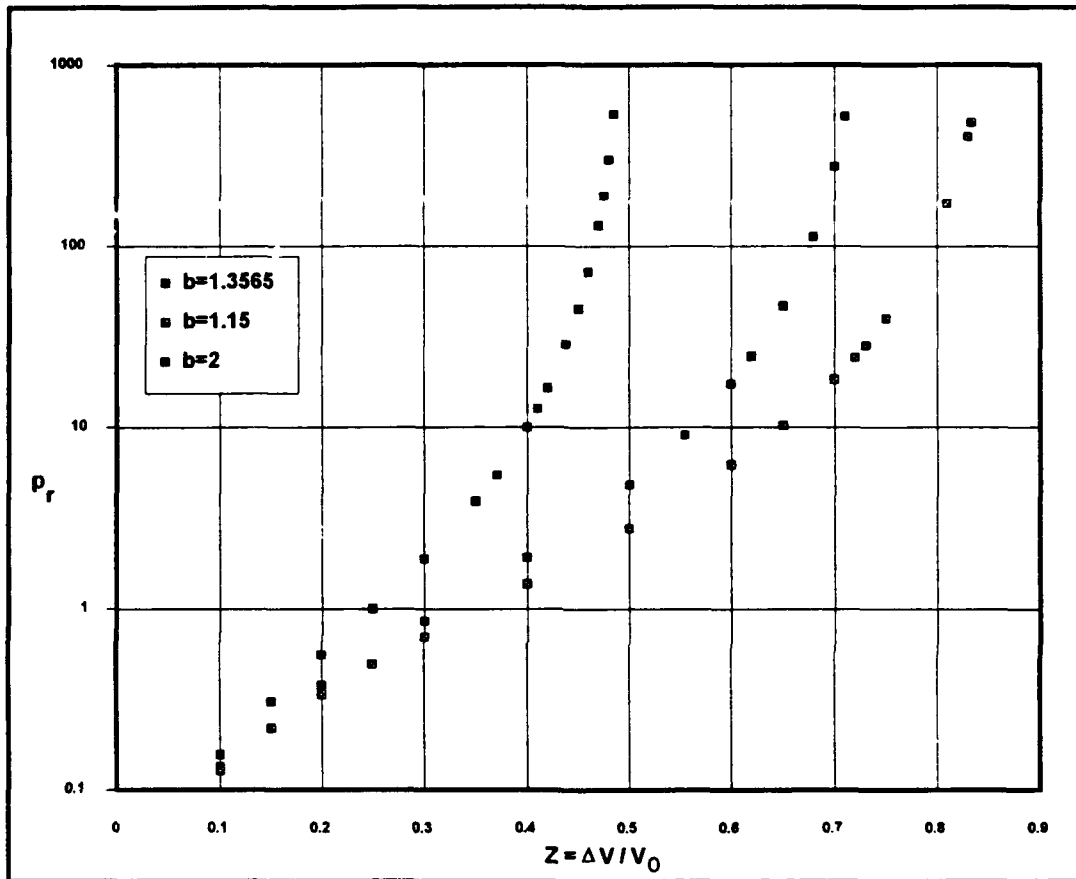


Figure 13. Reduced pressure versus compression,  $\Delta V/V_0$ , for three values of the slope of  $U_s - U_p$  curve.

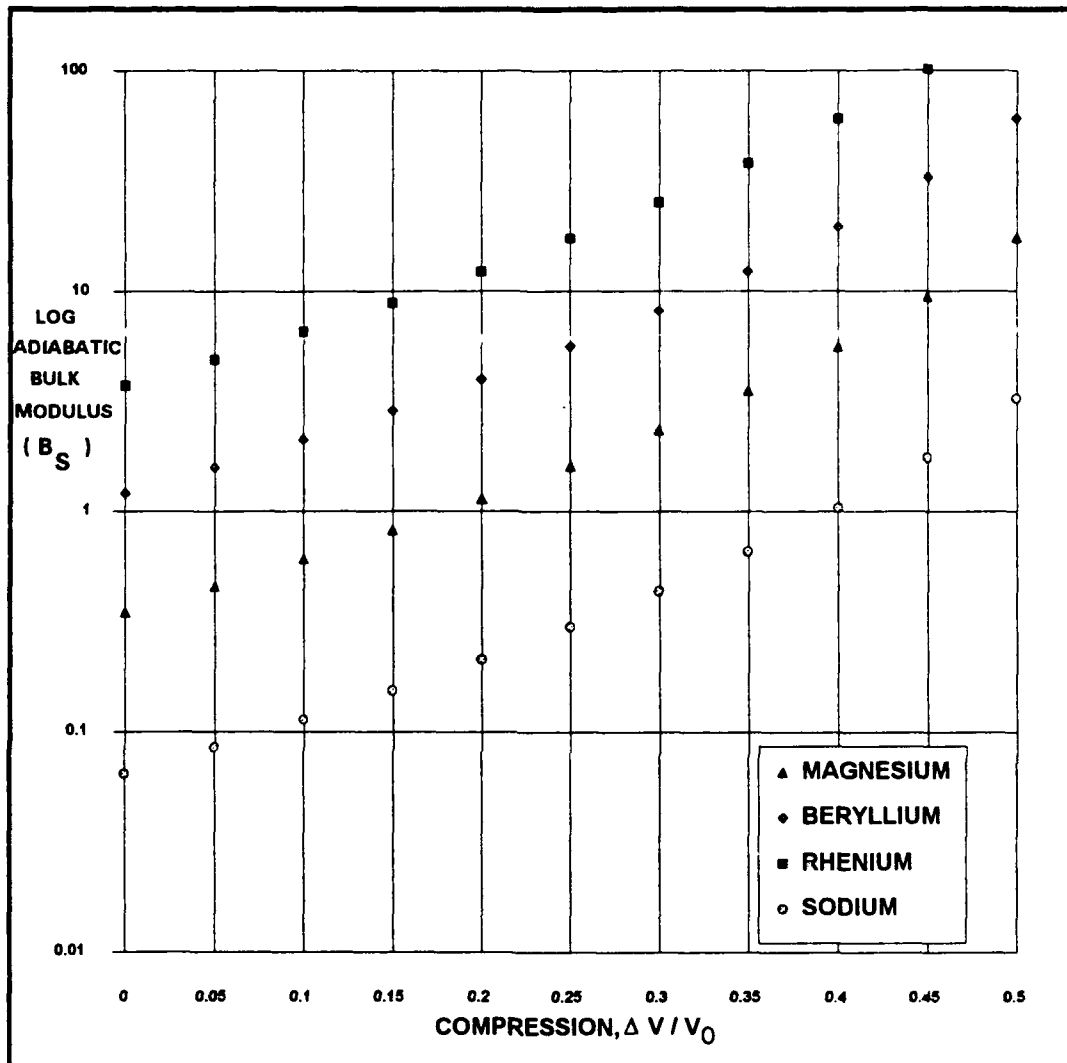


Figure 14. Adiabatic bulk modulus predictions for various compressions  $\Delta V/V_0$ .

dependence upon compression suggests that the interatomic forces that are responsible for resisting isothermal compression do not change much during adiabatic compression during a shock wave, except perhaps for temperature effects caused by the adiabatic heating. More importantly, if the isothermal bulk moduli have the same dependence upon the compression,  $Z$ , it is reasonable to expect that the adiabatic bulk moduli [to] have a similar behavior. If the values of  $s$  were as different as reported in the literature from independent statistical analyses, then one would expect a much larger variation in the dependence on  $Z$  than reported by Grover.

As can be seen from an examination of Table 1, the values of the slopes obtained by Slater and Dugdale using static values of the Grüneisen Constant compare with the universal slope derived from the  $U_s$  versus  $U_p$  line for various materials shown in Figure 9. The calculated values of the Grüneisen constants depend upon which equation is used. However, regardless of the source, either Slater or Dugdale predict a single value of the Grüneisen constant if all materials have the same slope.

The Grüneisen constant may also be temperature dependent (Ref. 9). Consequently, during a shock event, one would expect the volume and the temperature will change, which may explain why only the Grüneisen constants obtained only from shock tests do not agree with those obtained from either theory or from isothermal tests. After all, the adiabatic bulk modulus does not equal the isothermal bulk modulus. Since Equation 1 uses the Grüneisen constant to predict the Hugoniot of homogeneous materials, the evaluation of shock data presented above strongly suggests that shock experiments yield a single value for the Grüneisen constant for all materials.

## 5.2 PRIETO'S EQUATION OF STATE

In reviewing the work of Prieto (Refs. 7-11) presented in Section 3.0, the results presented in this paper are not new or surprising. Prieto developed a set of equations which are essentially the same as the variables in this study. Table 2 compares the variables used in this study, normalized by  $c$  and Prieto's reduced variables based upon the principle of corresponding states.

Table 2. Comparison of variables.

Variable	Present work	Prieto
Pressure	$P/C^2$	$P/(C^2)/s$
Shock Velocity	$U_s/C$	$U_s/C$
Particle Velocity	$U_p/C$	$U_p/(C/s)$
Compression Limit	$(s-1)/s$	$1/Z$
Energy	$E/(C/s)^2$	$E/(C/s)^2$

From Table 2, one concludes that the reduced variables approach used by Prieto and this work are fundamentally the same. One major difference is in the normalization of the pressure. In normalizing the pressure, Prieto (Ref. 8) calculates a reduced pressure based upon Equations 15 through 18 which contain a variable slope for the  $U_s$  versus  $U_p$  lines for different materials. However, this work suggests that the slope,  $s$ , is a constant, 1.35, for all materials and not a material parameter as was previously thought. A comparison of the experimental value of the reduced pressures using Equation 15 to Prieto's calculated value of the reduced pressure using Equation 12 shows the differences between the two methods. The results of this comparison are shown in Figure 15. It is worthwhile to point out that the universal slope, 1.35, shows an almost perfect correlation to the equation whereas the values used by Prieto consistently overestimate the reduced pressure.

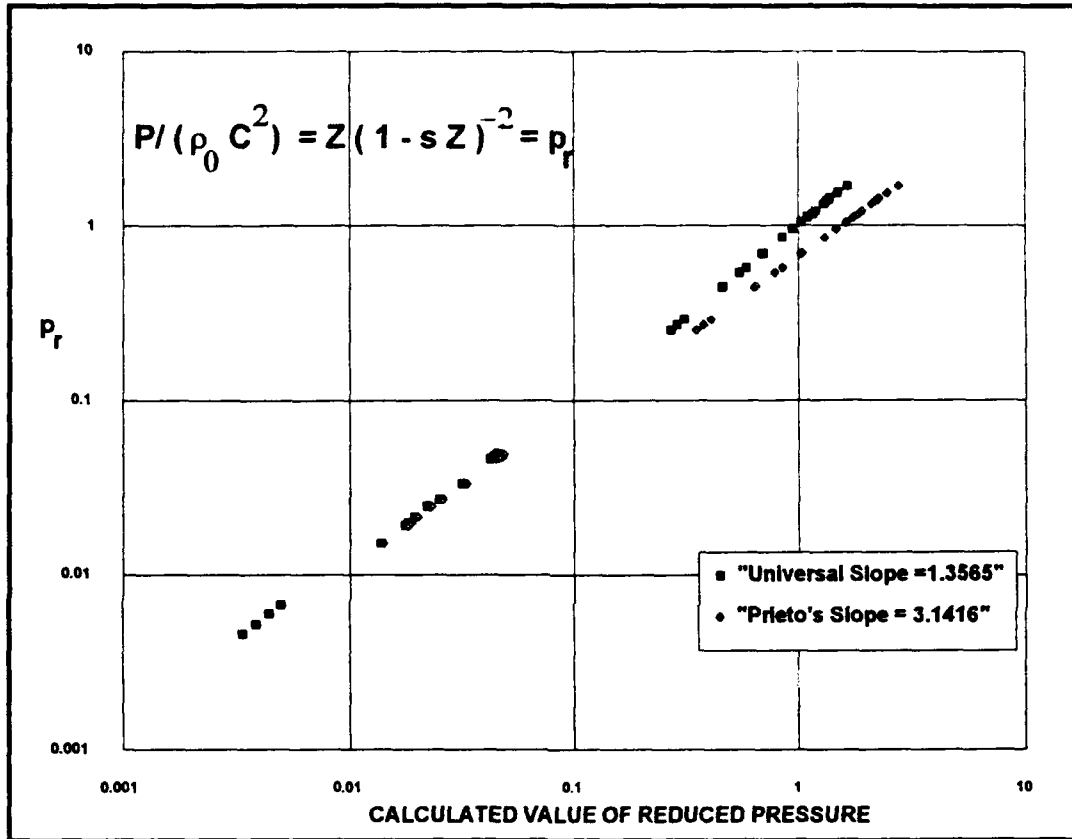


Figure 15. Comparison of master plot to Prieto's equation.

## 6.0 CONCLUSIONS

The development of a universal equation of state for all materials would appear to be a step closer than previously thought. The data seem to support a universal slope for the  $U_s$  versus  $U_p$  line which becomes even more significant at particle velocities near the speed of sound. The existence of a universal slope means that the material during shock can be represented by corresponding states. Thus, conventional thermodynamic variables such as pressure, volume, energy, etc., can be expressed as reduced or normalized variables as developed by Prieto (Ref. 9).

The correlations presented above establish a single equation for reduced pressure in terms of reduced particle velocity (Eq. 8) and a single slope for the  $U_s$  versus  $U_p$  line (Eq. 6) which is valid for all homogeneous classes of materials. It follows then that one could use these equations to predict the thermodynamic behavior of materials during shock even in the absence of shock data.

Finally, these results suggest that the force-distance behavior during compression is fundamentally the same for all materials, and the behavior of materials during shock appears to be largely a result of forcing the atoms, molecules, or ions together. Indeed, the literature implies that a single equation can be used to describe the force-distance behavior of ionic solids. The force-distance equations for metals, polymers, and covalent solids with less known force-distance potentials remain to be more fully explored. However, the shock compression described above suggests that all materials behave similarly. If the nature of the repelling forces is fundamental, one would expect materials to exhibit a response similar to the compression described above. The implication is that the change in the bulk modulus for all materials is the same for equivalent compression. Thus, the use of hydrodynamic codes to describe the shock propagation in all solid materials is supported by the results of the present work. In fact, except for the problem of the shear component of the sound velocity, the correlation of water with solids would seem to support the notion that the behavior of a solid under shock compression is fundamentally similar to that of a liquid.

## 7.0 FUTURE WORK

These conclusions need to be examined further. However, assuming that the universal slope concept is correct, the next point is how to apply the results to failure of homogeneous and nonhomogeneous materials during shock. Even if this analysis predicts adequately the response of materials to shock, it says little about damage mechanisms. The creation of dislocations, cracks, and voids in the microstructure of metals after shock is well known and appears to occur as a result of tension waves caused by reflections at the free surfaces, at interfaces, and at discontinuities in metals.

The use of the shock physics to predict spall is still elusive. If the damage is the result of relaxation phenomena, most of what is known can be used to predict the metal response once the stress/strain conditions are defined. However, the tools for making these kinds of predictions in the next generation of spacecraft materials are missing. Both polymer-based fiber-reinforced composites as well as particulate-hardened metal-matrix composites are much more complex than most materials studied to date. The presence of matrix-fiber or matrix-particle interfaces may disperse the shock waves as a stone dropped in a still lily pond initiates ripples which reflect off the lily pads. The interfaces between the matrix and the particles would act as shock wave reflection sites and would produce tension waves reflecting back from each interface. For example, the presence of microvoids in Al 6061, after sending a shock wave into a specimen, demonstrates the effect of metal-precipitate interfaces. In this experiment microvoids appeared at the precipitate interfaces. These observations for Al 6061 suggest that the damage caused by shock waves in nonhomogeneous materials, such as composites, may produce considerable separation at interfaces between the matrix and the second phase material. Thus, it is recommended that further tests are needed to define shock wave propagation behavior in nonhomogeneous materials. There is a special need to verify whether the behavior obeys the reduced variable correlation shown for other materials (Figs. 1-7) and whether the slope of the  $U_s$  versus  $U_p$  developed for homogeneous materials (Fig. 9) applies to nonhomogeneous materials. Finally, there is a need to characterize the damage that results from shock wave propagation in composites, especially with reference to the effect of particulates or fibers.

## REFERENCES

1. Walsh, John M. and Christian, Russell H., "Equation of State of Metals from Shock Wave Measurements," The Physical Review, 97, No. 6, pp. 1544-1556, March 15, 1955.
2. McQueen, R.C. and Marsh, S.P., "Equation of State for Nineteen Metallic Elements from Shock-Wave Measurements to Two Megabars," Journal of Applied Physics, 31, No. 7, pp. 1253-1269, July 1960.
3. Kohn, Brian J., Compilation of Hugoniot Equations of State, AFWL-TR-69-38, Air Force Weapons Laboratory, Kirtland AFB, NM, April 1969.
4. Slater, J.C., Introduction to Chemical Physics, Chapter 14, McGraw Hill, New York, NY, 1939.
5. Dugdale, J.S. and MacDonald, D.K.C., "The Thermal Expansion of Solids," The Physical Review, 89, p. 832, February 1953.
6. Alder, B., "Experiments With Strong Pressure Pulses," Solids Under Pressure, eds. W. Paul and D.M. Warschauer, McGraw-Hill, New York, NY, 1963.
7. Prieto, F., "A Law Of Corresponding States for Materials at Shock Pressures," Journal of Physics and Chemistry of Solids, 35, pp. 279-286, 1975.
8. Prieto, F.E. and Renero, C., "The Equation of State of Solids," Journal of Physics and Chemistry of Solids, 37, pp. 151-160, 1976.
9. Prieto, F.E. and Renero, C., "Equation for a Shock Adiat," Journal of Applied Physics, 41, p. 3876, 1970.
10. Prieto, F.E. and Renero, C., "Reduced Hugoniots," Journal of Applied Physics, 42, p. 296, 1971.
11. Rineto, C., Prieto, F. E., and del Daza, M., "Comparison of Two Universal Equations of State for Solids," Journal of Physics: Condensed Matter, 2, p. 295, 1990.
12. Pitzer, K., "Corresponding States for Perfect Liquids," The Journal of Chemical Physics, 7, pp. 583-590, August 1959.
13. Dymond, J.H., "Corresponding States: A Universal Reduced Potential Energy Function for Spherical Molecules," Journal of Chemical Physics, 54, No. 9, p. 3675, May 1971.

14. Grover, R., Hoover, W., and Moran, B., "Corresponding States for Thermal Conductivities Via Nonequilibrium Dynamics," Journal of Chemical Physics, 83, No. 3, pp. 1255-1259, August 1985.
15. Abbott, M.M. and Van Ness, H.C. , Thermodynamics, McGraw-Hill, New York, NY, 1972.
16. Grover, R., Getting, I.C., and Kennedy, G.C., "Simple Compressibility Relation for Solids," Physical Review B: Solid State, 7, No. 2, pp. 567-571, January 1973.